BEST: International Journal of Management Information Technology and Engineering (BEST: IJMITE)
ISSN (P): 2348–0513, ISSN (E): 2454–471X
Vol. 9, Issue 2, Dec2021, 119–130

UAV IMPACT MODELLING, SIMULATION AND ANALYSIS ON THE BASE OF MATERIAL VARIATION

TAFADZWA GERALD KAPESA, AYUBU JACKSON SAITABAU, SU-YAN & T. DMYTRO
Department of Civil Aviation, Nanjing University of Aeronautics and Astronautics, Nanjing, China

ABSTRACT

Unmanned Aerial Vehicles are rapidly increasing as the need for them in a vast array of applications such as traffic control, forest fire monitoring, earthquake monitoring, and military applications increases. This growth however, has also brought about collision while airborne between manned and the unmanned aircrafts and the damage severity ranging from minor deformation to a completely perforated aircraft structure. The recent comparison is the bird strike but the UAV has different material composition with a higher stiffness as compared to the soft tissue and bone of the bird. In this paper the analysis of different materials influence on the result of the strike was done and their effect on the severity on aircraft structure. The materials are, steel, aluminum, titanium alloys and polyamide. FEM is the method we use to depict the most dangerous materials through ABAQUS EXPLICIT simulation.

KEYWORD: Structural Material, UAV, Collision, FEM Analysis.

1. INTRODUCTION

The development in the UAV industry has spread out to many fields for instance entertainment, emergency rescue, environmental monitoring, power line inspection, and aerial mapping to name few. The market is of this development is expected to plummet to a total economic impact of $82.1 billion by the end of 2025[1]. The increase in UAV has resulted multiple incident such as the DJI Phantom 4 collided with an army UH-60M helicopter ,a Beech King Air A100 from Canada both verified incidents taking place in 2017 and the most recent a Cessna struck by a UAV in midair collision [2][3][4].The directives as per EASA the UAV airworthiness objective are to focus on understanding through experiment testing and simulation with target identify design strategies to mitigate risk. Experimental testing is expensive while simulation through FEM which is a more efficient and cheaper method in comparison [5]. The UAV design requirement is high precision and accuracy during flight for this its mandatory to have a high strength to weight ratio, material requirement should be aerodynamic and easily formed or shaped. The requirements balance also contributes to severity of impact damage as the material properties such as strength, elasticity and mass to name few. In this paper the material variation will show the most dangerous material through kinetic energy comparison and deformation on a plate.

Research Objectives

This article will focus on the different impact of structural material variation and how the effects of the properties can pose danger during the collision. The results of the severity to impact collision will be based on the kinetic energy, structure and shape of object before and after collision. Taking into account weight distribution, material stiffness of both object and also impact speed. And Altitude will not be of any effect so we consider it negligible. This is to contribute towards the airworthiness requirement for unmanned aircraft and manned aircraft and the damage severity to the impact while collision takes place in the airspace. Penetration in to the UAV has different levels as it enters through the skin which may cause part failure depending how severe the skin fracture extends [8].

Nomenclature

E Young's Modulus

V Poisson's Ratio

A, B, C, n, m Material constants of JC material model

Tr Room Temperature

Tm Melting Temperature

$\bar{\sigma}$ Equivalent Plastic stress

$\bar{\varepsilon}$ Equivalent Plastic strain

$\dot{\bar{\varepsilon}}$ Reference Equivalent Plastic Strain

ρ Density

Abbreviations

UAV Unmanned Aerial Vehicle

MSL Mean Sea Level

FE Finite Element

FEM Finite Element Method

EASA European Union Aviation Safety Agency

TC4 Ti-6AI-4V

PA6 Polyamide 6

FAA Federal Aviation Administration

ALLKE Kinetic Energy for Whole Model

ALLDMD Damage Dissipation Energy for Whole Model

2. MATERIAL SELECTION

Table 1: Material properties AL 2024-T53

Material	Density GPa	Young's modulus E	Poisson's Ratio	A	B	c	m	n
AL 2024-T3	2.77	73.1	0.33	368	683	0.04025	0.73	0

The Al 2024 from the duralumin series alloys available in plate form its alloy features has excellent mach inability, good workability, high strength and through cladding can it can resist corrosion. The properties combined make suitable to be used in aircraft structures such as ribs, fuselage structures and other places where stiffness is required.

Aluminum alloys are vital to aerospace manufacturing and their less flammable property makes them more popular as they contain magnesium. Along with a blend of some alloys, aluminum can be made high resistance to corrosion and improved desired properties which is another requirement of optimum design of UAV.

The Johnson cook's formula the known as (J-C) phenomenological constitutive model is the most utilized and is common in most of the commercial FE codes [12].

$$\bar{\sigma} = (A + B\varepsilon^{-n})\left[1 + C\ln\left(\frac{\dot{\varepsilon}}{\dot{\varepsilon_0}}\right)\right]\left[1 - \left(\frac{T - T_{room}}{T_m - T_{room}}\right)^m\right] \quad (1)$$

From eq (1) A, B, C, m and n are material parameters which are determined based on the stress data obtained from mechanical test. As mentioned by Guo and Horstemeyer [13], although this model is easy to apply and can describe the general response of material deformation, these effects are fundamental to proper modeling the surface integrity of machined components, including the residual stress distribution [13].

Table 2: Material Properties for Stainless Steel

Material	Density	Young's Modulus	Poisson's Ratio	A	B	C	m	n	Epsilon dot Zero
Stainless steel 321	7.91	193	0.27	280	1215	0.031	0.43	0	

Steel Alloys are valuable for the durability, hardness and resistance to high temperatures these properties make it suitable for aircraft skin, hinges and other parts. It makes 13% of the modern aircraft composition. The stainless steel is corrosion resistant that's is why it's applied on many aviation part [10].

Table 3: Material Properties for Ti-6Al-4V

Material	Density	Young's Modulus	Poisson's Ratio	A	B	C	n	m
Ti-6Al-4V	4.42	110	0.34	860	683	0.033	0.47	1.02

Titanium alloys are great with weight saving, heat resistance, resistance to embrittlement at low temperature, has very high corrosion resistance and low-thermal expansion. Commercially pure titanium is used for airframes where formidability is considered important.Ti-6Al-4V is formidable and has high strength to weight ratio.

Table 4: Material Properties for PA6

Material	Density	Young's modulus	Poisson's Ratio
PA6	1.17	4.20	0.36

Plastic PA6 is high strength and stiffness at high temperature also possesses good impact strength at low temperatures. The processing is very easily done to acquire good abrasion and wear resistance together with fatigue resistance. The polyamide can be compared with metals as they are formidable

Table 5: Shell value Tthickness vs Yield Stress.

Material	AL 2024-T35	Ti-6Al-4V	Stainless Steel 321 (UNS S32100)	Polyamide 6 (PA6)
Yield Stress	400-600	600-800	1200	0-200
Shell thickness (mm)	0.2	0.4	0.8	0.1
Shell thickness within requirement	2	1.3	1	4

The values for the thickness is lower than the standard requirement in order to absorb damage and increase stiffness. AL 2024-T35 and PA6 greater than 2mm and Ti-6Al-4V and Stainless Steel greater than 1mm.

3. AIRCRAFT STRUCTURE

The application of Aluminum alloys on the aircraft structure has been primarily catered for airframes after the 1920s. Their favorable as there are lightweight metal structures and low cost and easily manufactured. Cast alloys such as the selected 2024 alloy is used for its high performance and the strength it possesses especially in the application on the fuselage skin [15] [14]. The skin covers most of the aircraft area protecting the interior which if it collapses most problems occur and According to Gaisin Al2024-T3 is mostly used in the fuselage skin and lower wings of the aircraft where the fracture toughness. The required thickness is greater than or equal to 0.8mm. According National Transport Safety Board the required skin thickness is over 0.899mm as lesser will be vulnerable to impact damage from foreign objects especially at high speed and altitudes.

4. UAV MODELLING

Reverse engineering need is to design documentation of product, re-designing a product, design change in a product and increasing manufacturability of the product. It's very effective as it cuts out the time and cost of changing prototypes as you may do or changes within a matter of time. The revise model is scanned using laser scanners and structured light scanning instrument which are the two different lights used. Using CATIA V5 each part is reversed engineered.

The modelling takes place in figure 1(a) shape digitized shape editor where a planar section is created from the imported stl file figure 1(b). It is then traced as the figure 1(c) below shows the trace line which is the section reference line for the Lithium Polymer (Li-Po) battery cell [**Error! Reference source not found.**]. The pad is stretch to match the height of the battery figure 1(d) then the side feature sketch pad up to the stl visible depth figure 1(e). The battery is complete to a 3D model ready for assembly figure 1(h). The propeller steps are similar for figure 1(f) and (g). Power generated Surface is different as it accommodates the propeller curved surfaces, the edges are trimmed and the openings are closed to form a solid figure 1(I). Figure 1(j) and (k) are similar to the battery.

The whole model with other parts is assemble to form a complete 3D model and further mesh using Hypermesh.

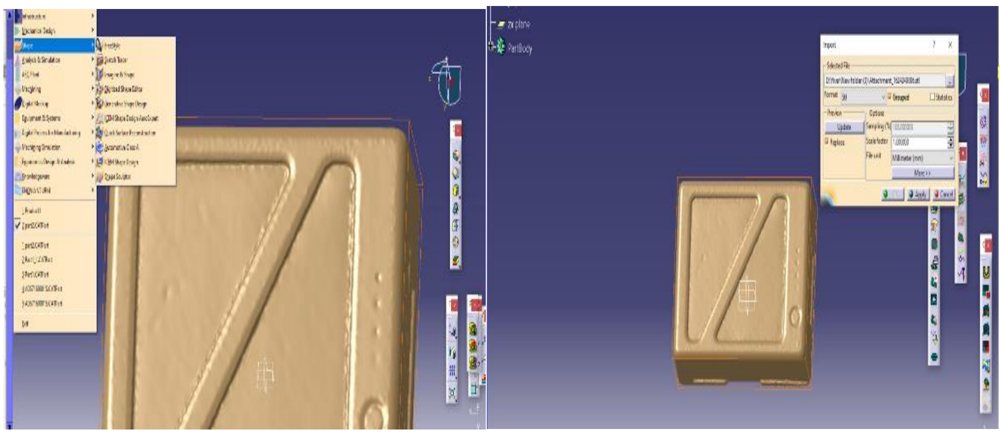

(a) **(b)**

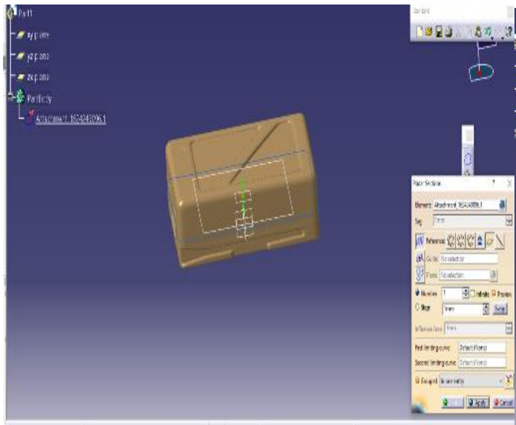
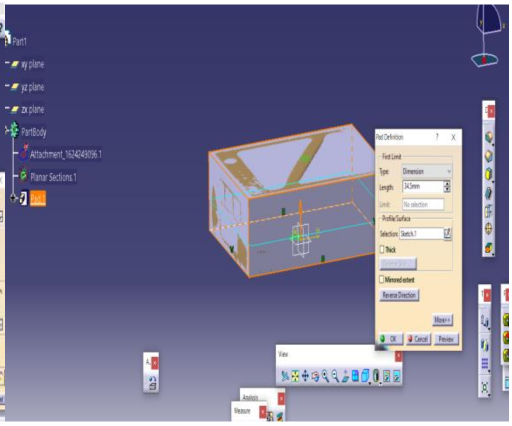

(c) (d)

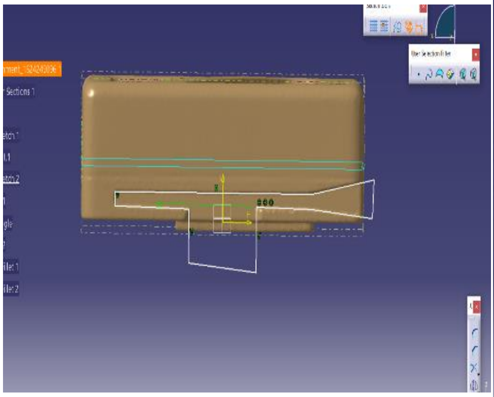
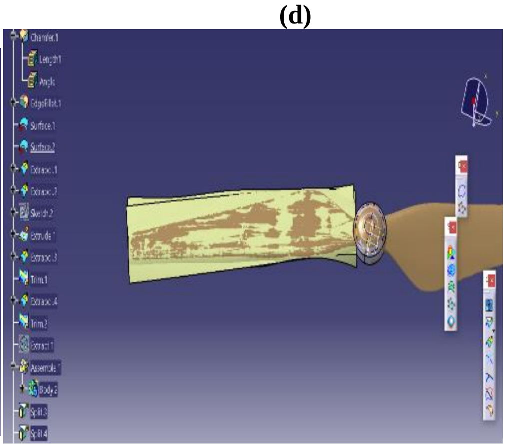

(e) (d)

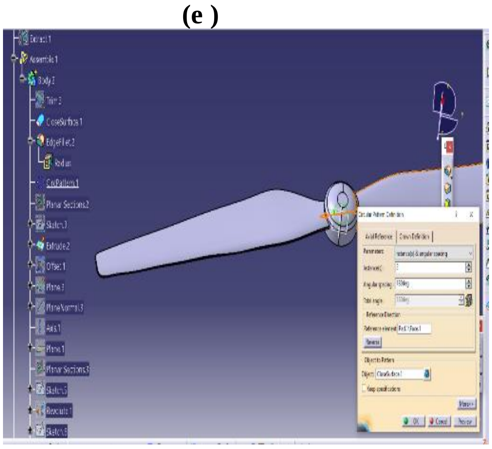
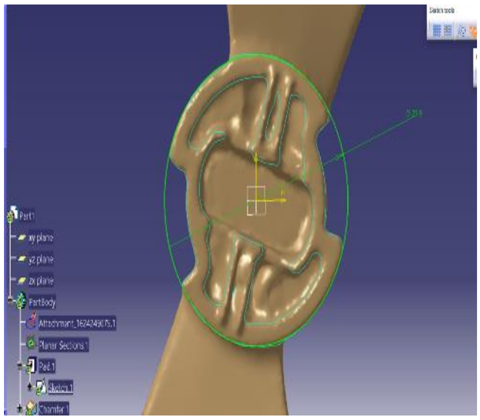

(f) (g)

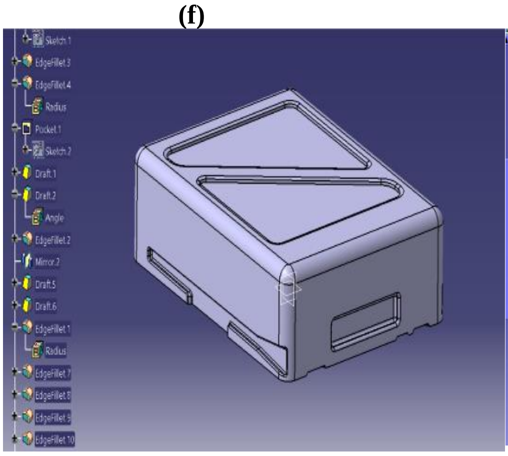
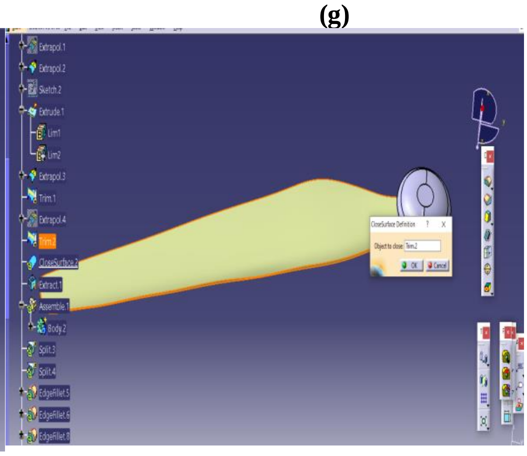

(h) (I)

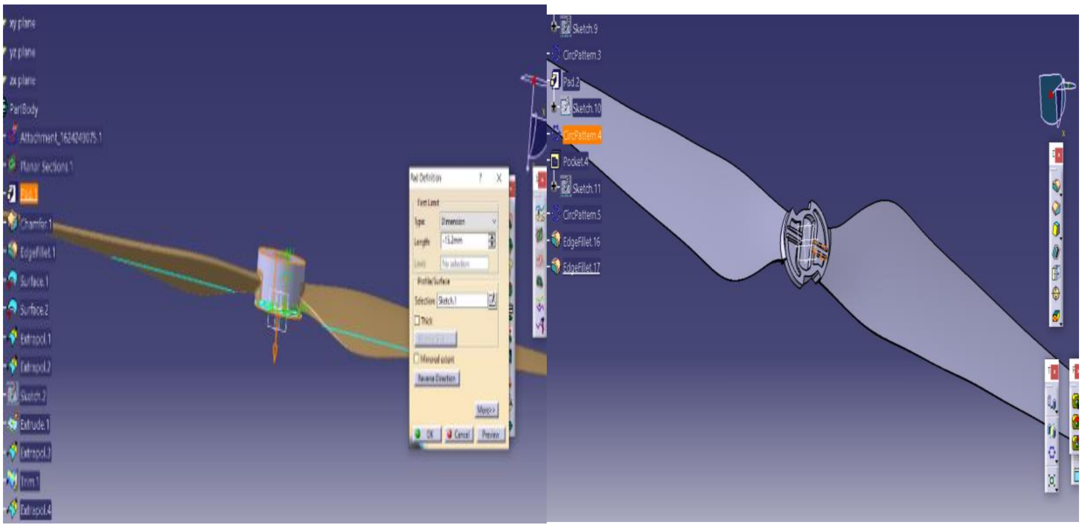

(j) (k)

Figure 1: Propeller and Battery Reverse Engineering.

5. DRONE AND AIRCRAFT COLLISION OPERATION CONDITIONS

The drone with a total weight of the batteries and the propellers included, m speed of 20m/s with max descending speed at 4 m/s and ascending 6m/s until 6000m maximum altitude and can sustain operation for half an hour before the next charge. The use for the drone is for surveillance and topographic recording and images in different industry sectors such as tourism or military application.

FAA regulation PART 107 states the drone is only allowed to fly below 121.92m, only higher if it's within 121.92m over a structure and maximum allowable speed at 100mph [6].

According FAR 91 117, no person may operate an aerial vehicle below 3048mMSL at an indicated airspeed of more than 65m/s [9].

The collision speed is the relative speed between drones and commercial aircrafts. The maximum flight speed of UAV is 72km/h [6]. The collision distance can be determined by superposition.

Table 6: Collision Point Velocity

Altitude	Aircraft Speed	UAV Speed	Relative Speed
121m	96m/s	20m/s	116m/s
500m	122m/s	20m/s	142m/s
65m/s	131m/s	20m/s	151m/s

6. MESH GENERATION

The mesh generation using hypermesh is a more refined form as the model will attain an accurate mesh in less time and flexibility to adjust or improve the quality of the mesh as per the requirement.

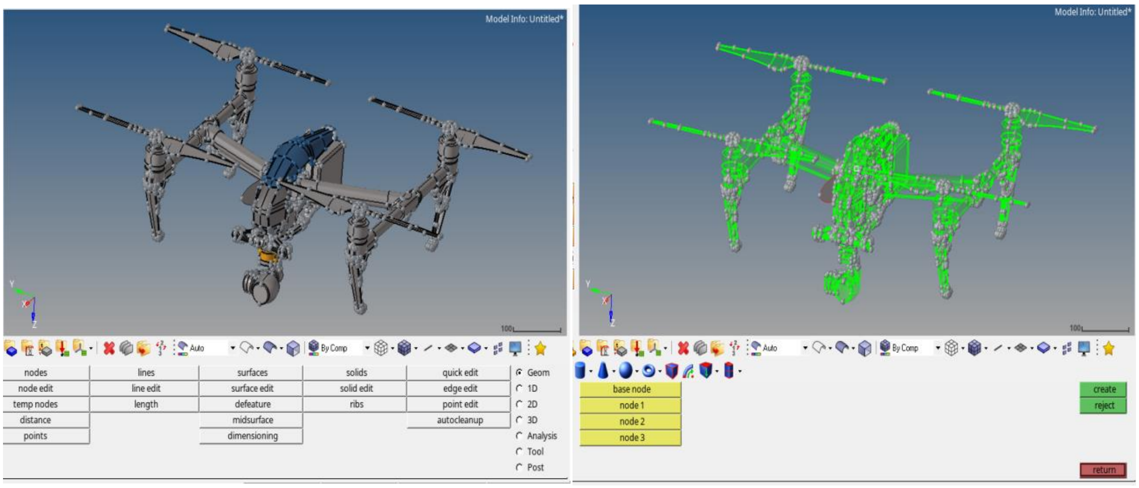

(a) **(b)**

Figure 2: Verification of Corrupt parts to Initiate Mmesh.

Using import option in the standard tab, import the geometry in hypermesh user interface dock figure 2(a). Selection of the file type from which it is saved preferably in iges format. After importing the model, the main step is to check how many components are available in hypermesh deck figure 2(b). The verification is done in order to check any part is corrupted or any part is missing while importing, this can be done by checking on left side panel in model tab figure 2(b). the components that are available in hypermesh deck. If any component is missing or corrupted, delete the file, the solution will be to go back to the parent file and import again. After selecting solids, the green color highlighted areas are visible. The highlighted areas with green color are considered as solids and the areas which are not highlighted are called as surfaces figure 2(b) and figure 3.

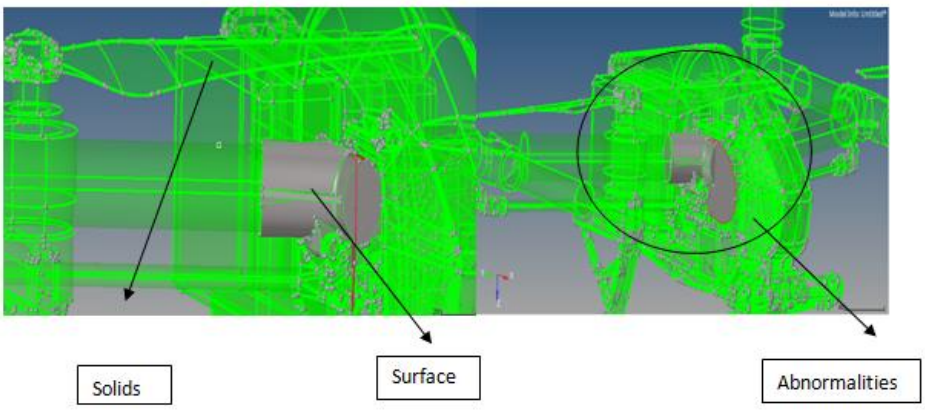

Figure 3: Checking and Removing Abnormalities.

Checking the Abnormalities in imported model as they are differentiated between solids and surfaces. Surfaces identify abnormalities that may affect mesh figure 3.

Selection of F11 option on the dock will open the interface above. After getting into this function, the surface is removed to delete the abnormal face as shown above figure 3.The verification of an errors is done and any other abnormalities shown can be removed and if none are the meshing commences as shown on figure 4(a}.

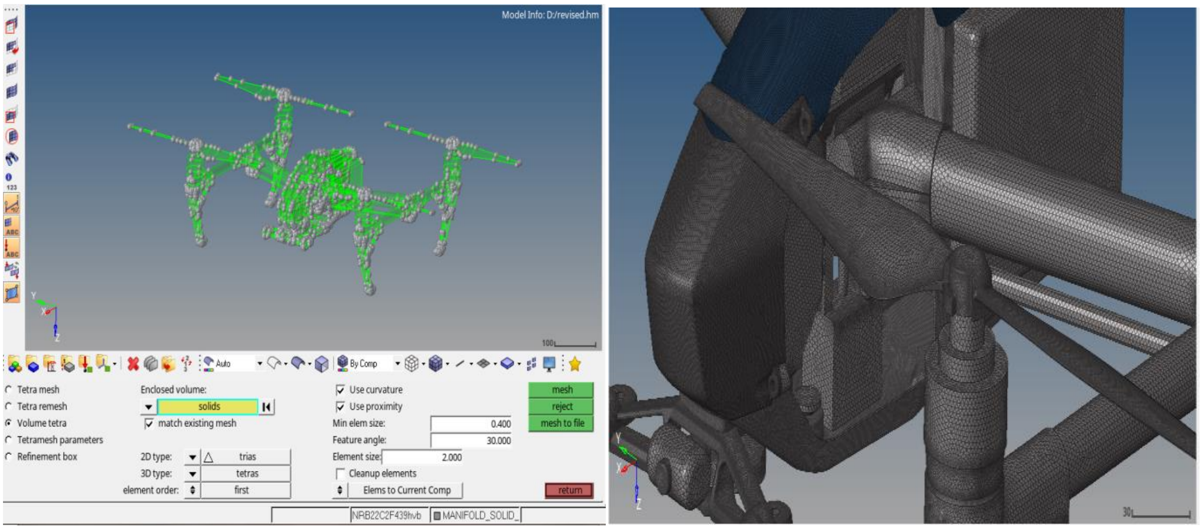

(a) (b)

Figure 4: Mesh Defeature Check and Mesh

The final part is the defeature check and the 3D tetra mesh is applied as model is ready with all parts meshed and connected. Volume tetra mesh for meshing the 3D model solids and enter element size 2 fig 4(a). The use curvature and use proximity for ease of meshing at the corners and fillets. While maintaining size 0.4 and feature angle and the mesh is generated at the simulation fig 4(b).

7. SIMULATION RESULTS AND ANALYSIS

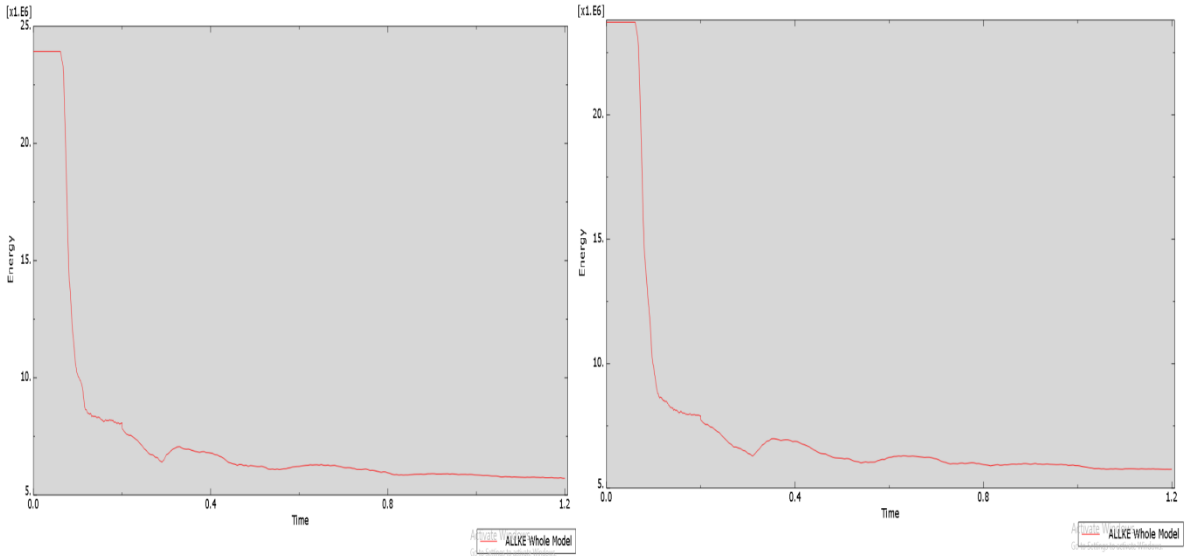

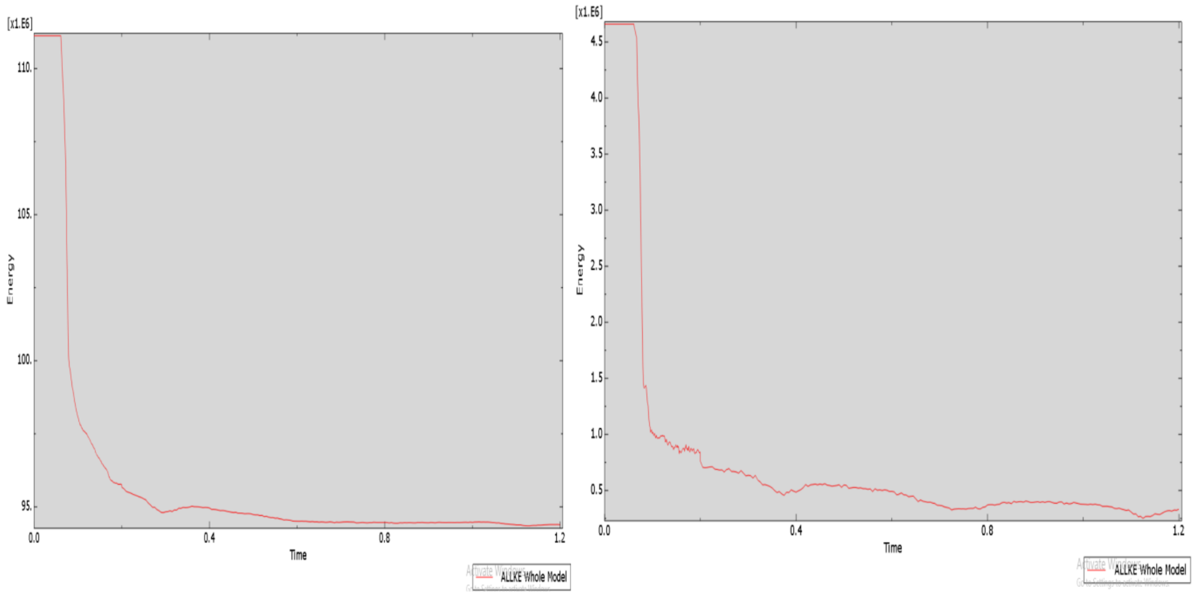

Figure 5: Kinetic Energy Graphs for the Drone Materials at 116m/s.

The ALLKE whole model graph show exponential decrease of the energy trend. When the drone contacts the plate the steel as mass is directly proportional to density. The aluminum compared to the titanium at contact the kinetic energy is higher because the shell thickness of the UAV is higher than that of Titanium although Ti-6Al-4Vmass density is greater as shown on table 3.

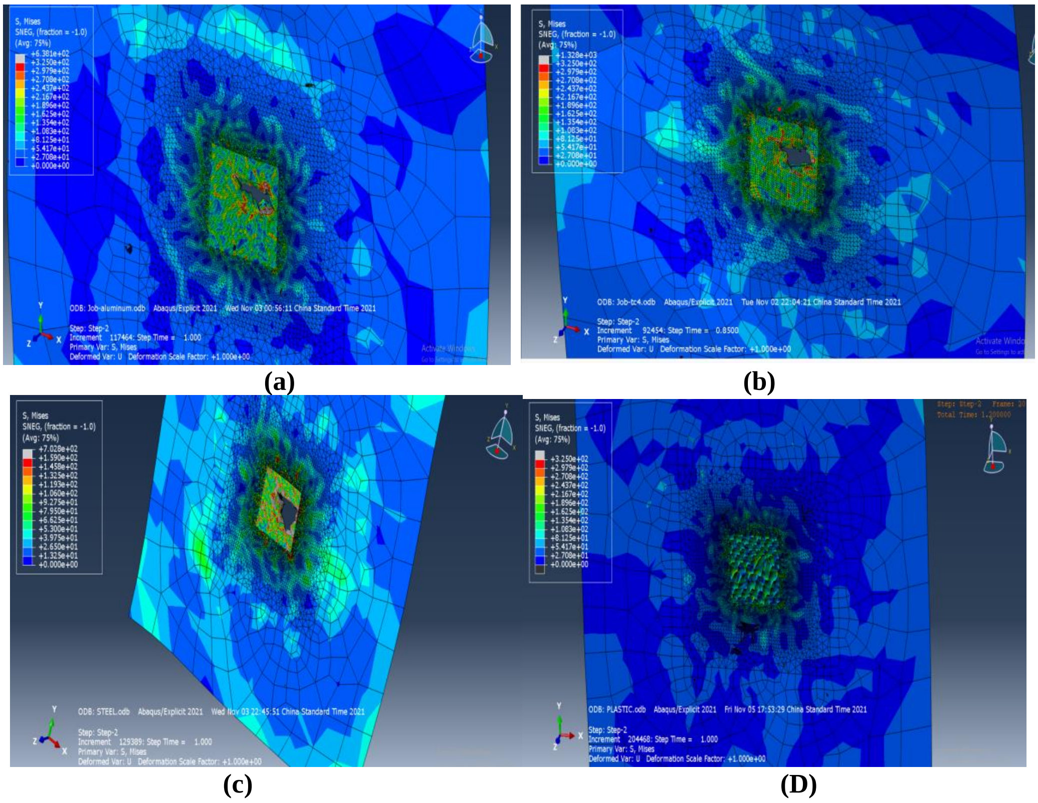

Figure 6: Von-Mosses Stress of the Different Material Applied at 116m/s.

The stress 1.328E+03MPa is for fig 6(b)Ti-6Al-4V has the highest compared to figure 6(c) stress maximum value of 7.028e+02 MPa Stainless Steel alloy of high density because of the shell thickness is less PA6 figure 6(d) has the least stress value as the density is less yet it has the highest shell thickness.

The ALLDMD Energy for the Four Materials at 116m/s

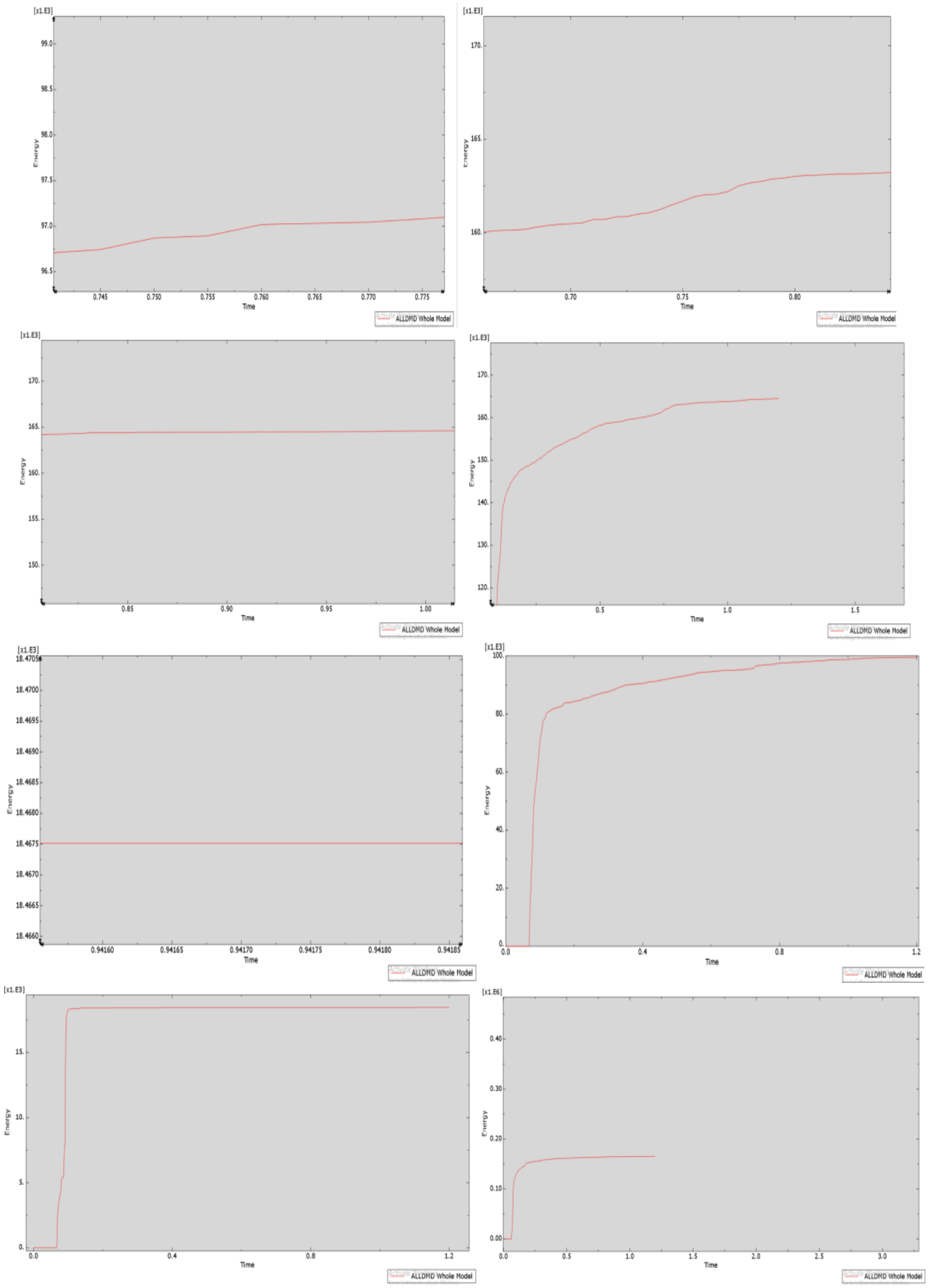

Figure 7: ALLDMD Energy Values for the Four UAV Materials.

ALLDMD Steel has the highest damage dissipation energy 1653e+03J followed Aluminum alloy has 160e+03J.Titanium has 97.25e+03J and finally the lowest DMD energy PA6 has 18.4670e+03J.

8. CONCLUSIONS

The results of the four drones impact against a AL 2024 T3 plate are shown in form of stress , kinetic energy and damage dissipation energy. The Kinetic energy exponential decrease exhibits trend comparatively the stainless steel drone has the highest because of greater mass which is directly proportional to the density shown on table 2.The drone with the AL 2024-T3 compared to theTi-6Al-4V at contact has more kinetic energy because the the shell thickness of the UAV is higher than that of Ti-6Al-4V although density is greater.The highest stress 1.328E+03MPa is for the Ti-6Al-4V UAV has the highest compared to Steel alloy drone of a higher density this is due the shell thickness value table 5 . The drone containing PA6 material proprties has the least stress value as the density and mass is the west however it has the highest shell thickness values shown on table 5 .The Stainless steel drone has a higher stress than the AL2024-T3.

ALLDMD Stainless Steel has the highest damage dissipation energy 1653e+03J. Aluminum alloy has 160e+03J lost energy. Ti-6Al-4Vhas 97.25e+03J and finally the lowest dissipation energy is PA6 has 18.4670e+03J. The damage of the PA6 does not penetrate the plate all though the UAV severely damaged while the other materials penetrate the skin and after the collision the UAV completely disintegrated.

REFERENCES

1. EASA, Drone Collision Task Force, Final Report 04-10-16, 2016
2. "Drone Hits Army Helicopter Flying Over Staten Island". WCBS-TV. 22 September 2017. Retrieved 26 September 2017.
3. "A first in Canada: Drone collides with passenger plane above Quebec City airport". CBC News. 15 October 2017. Retrieved 23 October 2017.
4. Wilson, Karissa (20 August 2021). "Plane damaged after being hit by York police drone at Buttonville Airport". CTV News. Retrieved 22 August2021.
5. Fonseca, P. Simulation hypotheses. In Proceedings of SIMUL 2011; 2011; pp. 114–119. https://www.researchgate.net/publication/262187532_Simulation_hypotheses_A_proposed_taxonomy_for_the_hypotheses_used_in_a_simulation_model
6. FAA, Small UAS, FAR 107,2016
7. E. Sahraei, J. Meier, T. Wierzbicki, Characterizing and modeling mechanical properties and onset of short circuit for three types of lithium-ion pouch cells, J. Power Sources 247 (2) (2014) 503–516.
8. British Military Aviation Authority, Small remotely piloted aircraft systems drone midair collision study, Report-16, 2016.
9. ASSRRE, UAS Airborne Collision Severity Evaluation of Quadcopter, 2017, Final Report II.
10. He, G. Xie, H. Zhang, et al., A comparative study on Johnson–Cook, modified Johnson–Cook and Arrhenius-type constitutive models to predict the high temperature flow stress in 20CrMo alloy steel, Mater. Des. 52 (24) (2013) 677–685.

11. S. Salehghaffari, M Raisrohani, Epistemic uncertainty modeling of Johnson-Cook plasticity model using evidence theory, in: AIAA/ISSMO Multidisciplinary Analysis Optimization Conference, 2013.
12. Johnson GR, Cook WH. A constitutive model and data for metals subjected to large strains, high strain rates and high temperatures. In: Proc. 7th Int. Symp. On Ballistics, Hague, Netherlands, April 1983; 541–547.
13. Guo YB, Wen Q, Horstemeyer MF. An internal state variable plasticity-based approach to determine dynamic loading history effects on material property in manufacturing processes, Int. J. Mech. Sci. 2005; 47: 1423–1441.
14. Verma, J. Atkinson and M. Kumar Bull Mater Sci, 24 (2) (2001), pp. 231-236
15. Campbell F.C. Aluminum, elements of metallurgy and engineering alloys ASM International (2008), pp. 487-508